Available online at www.sciencedirect.com
ScienceDirect
Journal of Power Sources 168 (2007) 184–190
JOURNAL OF POWER SOURCES
www.elsevier.com/locate/jpowsour

Improvement on the corrosion protection of conductive polymers in pemfc environmets by adhesives

J.G. Gonzalez-Rodriguez [a,*], M.A. Lucio-García [a], M.E. Nicho [a], R. Cruz-Silva [a], M. Casales [b], E. Valenzuela [c]

[a] *UAEM-CIICAP, Av. Universidad 1001, Col. Chamilpa, 62209-Cuernavaca, Morelos, Mexico*
[b] *Universidad Nacional Autonoma de México, Instituto de Ciencicas Físicas, Av. Universidad s/n, Col. Chamilpa, 62210-Cuernavaca, Morelos, Mexico*
[c] *Universidad Politécnica de Chiapas, Cuerpo Academico de Energía y Sustentabilidad Eduardo J. Selvas S/N, Col. Magisterial, Tuxtla Gutiérrez, Chiapas, Mexico*

Received 27 October 2006; received in revised form 19 February 2007; accepted 19 February 2007
Available online 27 February 2007

Abstract

The corrosion protection of polypirrol (PPY) and polyaniline (PANI) coatings electrochemically deposited with and without polyvinil alcohol (PVA) as adhesive onto 304 type stainless steel has been evaluated using electrochemical techniques. Environment included 0.5 M H_2SO_4 at 60 °C whereas employed techniques included pothentiodynamic polarization curves (PC), linear polarization resistance (LPR) and electrochemical impedance spectroscopy (EIS) measurements. Results showed that the free corrosion potential, of the substrate, E_{corr}, was made more noble up to 500 mV with the polymeric coatings. The corrosion rate was lowered by using the polymers, but with the addition of PVA, it was decreased further, one order of magnitude for PPY and up to three orders of magnitude for PANI. Impedance spectra showed that the corrosion mechanism is under a Warburgh-type diffussional process of the electrolyte throughout the coating, and that the uptake of the environment causes the eventual failure of the coating corroding the substrate.

Keywords: Conductive polymers; Corrosion; Sulfuric acid; Fuel cells

1. Introduction

Materials used in bipolar plates in polymer exchange membrane (PEM) fuel cells must have good mechanical properties, electrical and thermal conductivity and resist the corrosion produced by the acidic environment found, i.e. sulfuric acid (H_2SO_4) at 80 °C [1]. Conventional carbon steels show high corrosion rates, higher than the recommended corrosion rate for metal bipolar plates, 0.016 mA cm^{-2} [2] whereas stainless steels will passivate, protecting from corrosion, but leading to high contact resistance. Therefore, the options left are either using more noble or cheaper metals or protect them with inhibitors or conducting polymer coatings. Interesting possibilities for coating applications are offered by conducting polymers, which have received a great deal of attention in the last three decades [3–5]. Conducting polymers are considered to have technological potential to be used as coatings for corrosion protection.

Polypirrole (PPY) and polyaniline (PANI) coatings made by electropolymerization are often investigated to give high corrosion protection to metals such as iron and stainless steel [6–11]. In the case of PANI, however, a highly acidic environment is needed since there will be a competitive process between electrodeposition and metal oxidation, whereas PPY can be deposited from more neutral solutions. PPY has been shown to protect against corrosion for stainless steels and aluminum in different electrolytes [9] whereas PANI was proven to give protection in sulfuric acid (H_2SO_4) at 60 °C [13]. Lucio-Garcia and Smith [14] demonstrated that the use of additives such as dodecyl benzene sulphonic acid (DBSA) gave some improvement on the corrosion protection of 304 type stainless steel in 0.5 M H_2SO_4 at 60 °C only at the free corrosion potential. However, due to the loss of passivity of these samples, the corrosion

* Corresponding author. Tel.: +52 777 3329 70 84; fax: +52 777 3297084.
E-mail address: ggonzalez@uaem.mx (J.G. Gonzalez-Rodriguez).

0378-7753/$ – see front matter © 2007 Published by Elsevier B.V.
doi:10.1016/j.jpowsour.2007.02.039

Table 1
Conditions used for electrodeposition of the polymeric coatings

Coating system	Initial potential (mV)	Final potential (mV)	Solutions
PPY	−200	800	0.5 M H_2SO_4, +0.1 M of pyrrol monomer
PANI	−200	1000	0.1 M H_2SO_4, +0.1 M aniline monomer
PPY + PVA	−200	800	0.5 M H_2SO_4, +0.1 M of pyrrol monomer + 2 g of PVA
PANI + PVA	−200	1000	0.1 M H_2SO_4, +0.1 M aniline monomer + 2 g of PVA

rates in the potential range applicable to PEM fuel cells were either similar to or larger than the bare metal.

In this work, the effect of an additive such as polyvinyl alcohol (PVA) on the corrosion protection given by PPY and PANI to a 304 type stainless steel in 0.5 M H_2SO_4 at 60 °C, environment used in a typical PEM fuel cell is reported.

2. Experimental procedure

Bi-distilled aniline and polyvinyl acetate were used for polymeric coatings. Commercially available 304 type stainless steel sheets of 5 mm × 10 mm × 2 mm were used as substrates. They were abraded with 600 emery paper and degreased with acetone before the polymeric film covering process. PVA was prepared as solution by dissolving it in methanol.

A three-electrode electrochemical cell was used for electrodeposition of polymeric coatings. The reference electrode was silver/silver chloride, Ag/AgCl, and a platinum mesh was used as auxiliary electrode. 0.1 M sulfuric acid aqueous solution was used as the supporting electrolyte. Potential range for voltammograms was chosen between −200 and 600 mV at a scan rate of 20 mV s^{-1}. All experiments were carried out at room temperature. Single and composite polymeric films were obtained by cyclic voltammetry and the deposition process was always stopped at potential more positive than the oxidation potential to get an oxidized polymer. Conditions used are summarized in Table 1. Twenty cycles were used for electropolymerization. To obtain the PANI-PVA or PPY-PVA films 2 g of PVA was added into 100 ml of electrolyte.

Sulfuric acid (H_2SO_4) aqueous solutions in a concentration of 0.5 M was prepared with analytical grade chemical reagents. Potentiodynamic polarization curves were carried out by using an ACM Instruments potentiostat controlled by a computer at a scan rate of 1 mV s^{-1} in a three-electrode electrochemical cell with a saturated calomel electrode as reference electrode and a graphite rod as auxiliary electrode. The exposed area of the specimen was 1.0 cm^2. The polarization resistance (R_p) was evaluated by running linear polarization resistance (LPR) curves, which were obtained by polarizing the electrode from −10 to +10 mV with respect to the free corrosion potential, E_{corr}, at a scan rate of 1 mV s^{-1}. The tests lasted 24 h. The corrosion current, I_{corr}, can be calculated using the Stern–Geary equation [15]:

$$I_{corr} = \frac{b_a b_c}{2.3(b_a + b_c)R_p} \quad (1)$$

where b_a and b_c are the anodic and cathodic Tafel slopes, but, since in some cases it was very subjective to estimate b_a and b_c, we report R_p instead. Electrochemical impedance spectroscopy tests were carried out at E_{corr} by using a signal with an amplitude of 10 mV and a frequency interval of 0.1–100 kHz. A model PC4 300 Gamry potentiostat was used for this. All the tests carried out at 60 °C. Finally, surface morphology of the polymeric films, before and after corrosion tests, were analyzed in a Karl Seizz DSM100 scanning electronic microscope, SEM.

3. Results

3.1. Polymerization

Fig. 1 shows the cyclic voltammograms of the electrodeposition of polyaniline films onto stainless steel substrates. It illustrates two main oxidation peaks at about 420 mV (peak a) and about 860 mV (peak c), and a middle peak b at 560 mV. According to literature [16], peak a is due to the formation of radical cations (i.e. oxidation of the leucoemeraldine (LE) to emeraldine salt (ES)) whereas peak c corresponds to the subsequent oxidation of ES into the fully oxidized form of PANI, pernigraniline (PE). Peak b corresponds to the degradation of the radicals into benzequinone during the polymerization process. Counter peaks of a and c in the cathodic zone correspond to d (60 mV) and f (520 mV), respectively. Another oxidation peak starting at 800 mV which corresponds to the oxidation of aniline (generation of radical cations) was observed and takes place when the potential of the electrodes are raised up to 800 mV.

When the PANI + PVA films were electrodeposited (Fig. 2) it was observed that the oxidation and reduction peaks were

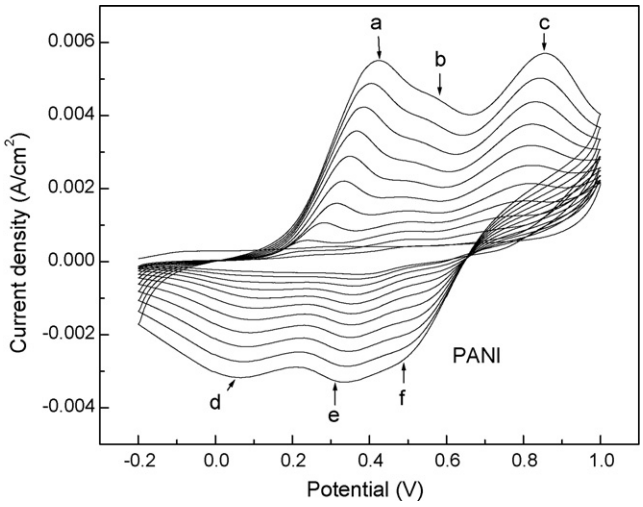

Fig. 1. Cyclic voltammogram of the electrodeposition of PANI.

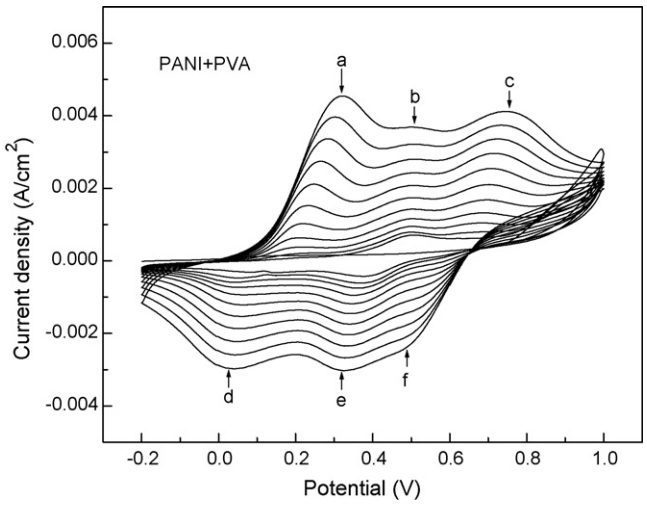

Fig. 2. Cyclic voltammogram of the electrodeposition of PANI + PVA.

shifted towards lower potentials (peak a at 300 mV, peak c at 750 mV, peak d at 20 mV and peak f at 510 mV), which means that during the electrodeposition of PANI–PVA the oxidation of aniline is given at lower potential than PANI films. At the same time, the corresponding maximum anodic and cathodic currents exhibited lower values than those PANI films, leading to a thinner PANI–PVA film. It seems that the incorporation of PVA acts to slow down the growth rate of the polymeric film.

3.2. Corrosion tests

Fig. 3 shows the polarization curves for uncoated 304 type stainless steel (304SS) and the coated 304SS with PANI, PPY, PANI + PVA and PPY + PVA after one hour of exposure to the 0.5 M H_2SO_4. Uncoated 304 SS has an E_{corr} value around −300 mV and an initial passivation interval between −200 and −100 mV, followed by a reactivation and then a fast repassivation. The passive current density was near 7×10^{-5} A cm^{-2}. Above 600 mV the current density starts to increase in a slow fashion, reaching a value of 1 mA cm^{-2} approximately at 800 mV. The presence of the polymeric coatings, for all cases, increased the E_{corr} values respect to that obtained for the bare metal for at least 100 mV (for the PANI + PVA film) and up to 500 mV (for the PANI coating). The corrosion current densities were lowered several orders of magnitude with these coatings. All the anodic current density values were in the passive range but higher than that for the bare metal; in these cases, reduction of the film as part of the mechanism of protection is not longer possible. There was an oxidative peak between 700 and 800 mV for the PANI and PANI + PVA films, due to the reversible oxidation of the films around these potentials. At higher potentials, the films are over oxidized and lost their conductivity.

The change in R_p with time for the different coating systems and the bare metal is given in Fig. 4. It can be seen that, during the first hours the R_p values for the coatings containing .PVA, were very similar to each other. After a few hours the PANI + PVA film had the highest R_p value, almost four orders of magnitude higher than that obtained for the bare metal followed by the PPY + PVA film. The R_p value for the uncoated metal and the films without PVA were very similar to each other throughout the tests, around 2×10^2 Ω, compared with 2×10^3 and 5×10^5 Ω obtained with PPY and PANI films with PVA respectively. Thus, the most protective coatings were obtained when the adhesive, PVA, was added to the polymeric films, especially to the PANI film.

Electrochemical impedance spectroscopy results in the Nyquist format for the uncoated 304 SS is given in Fig. 5 whereas the corresponding plots for the polymeric films are given in Figs. 6–9, respectively. From Fig. 5, we can see that the value of the diameter of the high frequency semicircle, the charge transfer resistance, R_{ct}, for uncoated 304 type stainless steel increases with time, which can be due to the establishment of the passive layer, as evidenced in Fig. 3. These plots show a charge transfer mechanism coupled to a diffusion controlled reaction, which may be due to the transport of reactants through the passive layer.

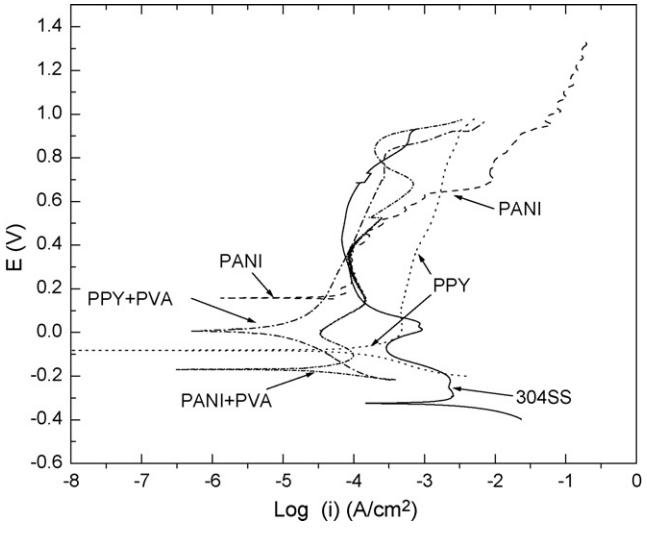

Fig. 3. Polarization curves for 304 type stainless steel with different polymeric.

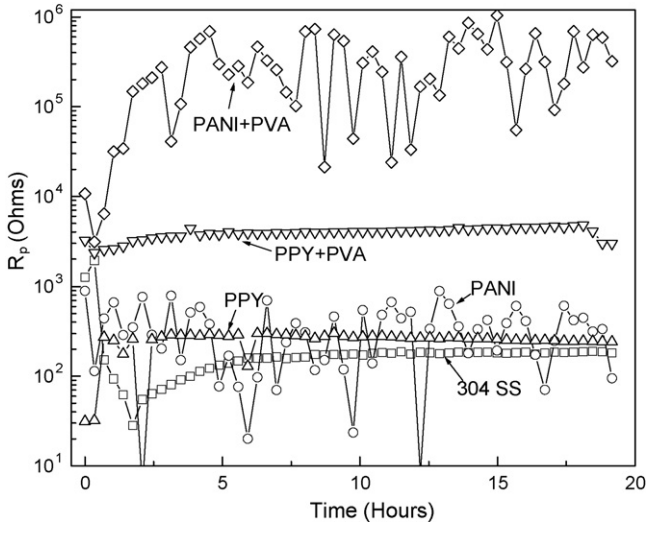

Fig. 4. Change in the R_p with time for 304 type stainless steel with different polymeric coatings.

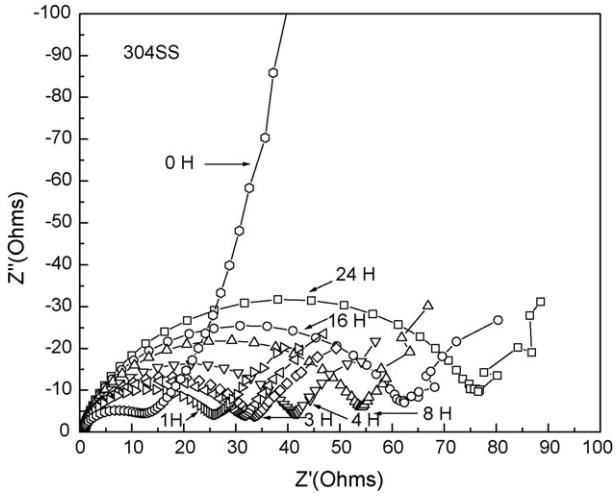

Fig. 5. Nyquist plots of the impedance spectra for uncoated 304 type stainless steel.

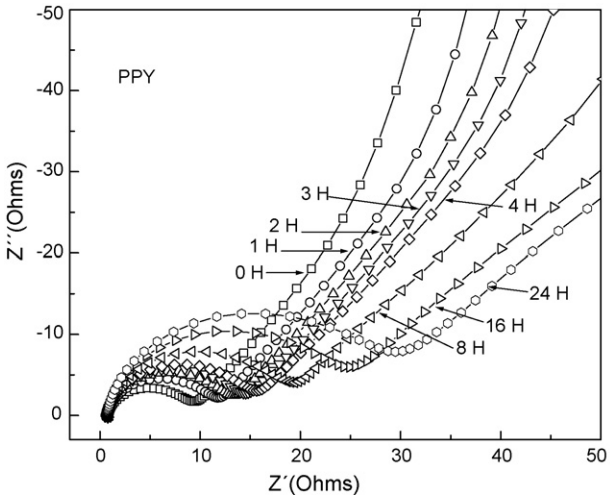

Fig. 6. Nyquist plots of the impedance spectra for the PPY coating.

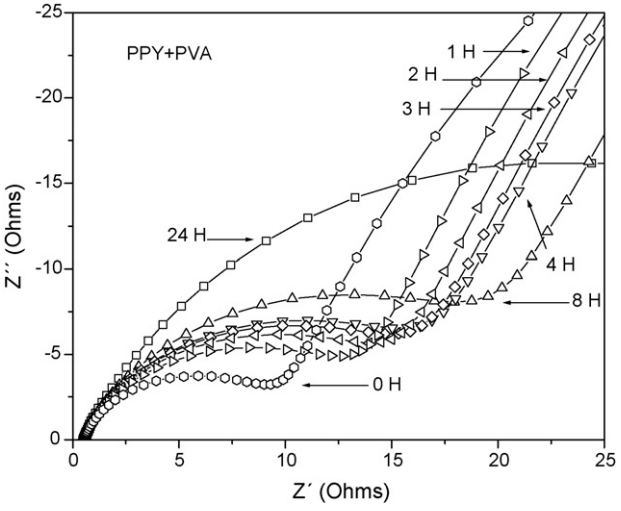

Fig. 7. Nyquist plots of the impedance spectra for the PPY + PVA coating.

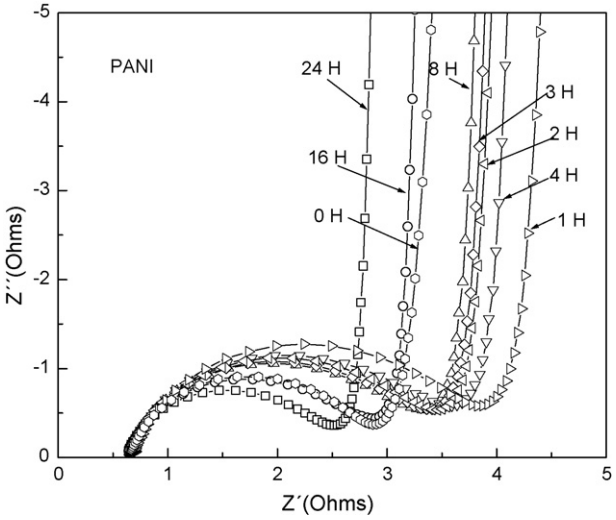

Fig. 8. Nyquist plots of the impedance spectra for the PANI coating.

This behavior was observed for all the coatings too, i.e. the diameter value of the high frequency semicircle, the charge transfer resistance, R_{ct}, increased with time. This value was lower than those obtained for bare stainless steel. For the PANI coating, however, the R_{ct} value decreased with time, whereas it remained constant for the PANI + PVA film. For instance, from Fig. 5, we can see that the R_{ct} value for the uncoated 304 stainless steel at the beginning of the experiment was 15 Ω and increases up to 80 Ω after 24 h of immersion. On the other hand, the R_{ct} value for the PPY polymeric film (Fig. 6) at the beginning of the test was around 10 Ω and increases only up to 30 Ω after 24 h of immersion. The R_{ct} values for the PANI-containing coatings were the smallest ones. As we will see bellow, this reduction in the R_{ct} values for the polymeric films respect to those values obtained for the uncoated 304 stainless steel is attributed to the high conductivity of the polymeric films.

A metal oxide layer is often described by a Voigt element that can be represented by a resistance and a capacitance in parallel. The same method can be used for the polymeric film. In

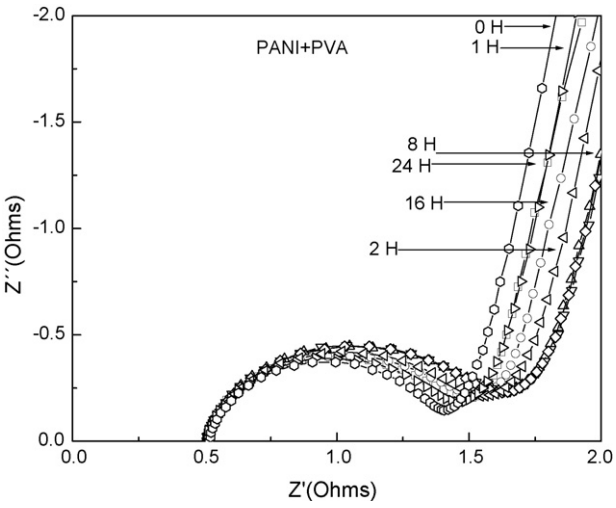

Fig. 9. Nyquist plots of the impedance spectra for the PANI + PVA coating.

a Faraday reaction, its rate is controlled by ion transfer from the conductive polymer, in our case, and a Warburg impedance. The double layer at the polymer film can be represented by a capacitance. Thus, the following elements are to be expected in the equivalent circuit model: R_{ct} represents the charge transfer resistance of the polymer film reaction; W represents the Warburg impedance and C_{dl} represents the double layer capacitance associated with the polymer/solution interface; finally, R_s represents the solution resistance. However, one has to account for the inhomogeneity of the polymeric film coating system. When a non-ideal frequency response is present, it is commonly accepted to employ distributed circuit elements in an equivalent circuit. The most widely used is constant phase element (CPE), which has a non-integer power dependence on the frequency. The impedance of a CPE is described by the expression:

$$Z_{CPE} = Y^{-1}(jw)^{-n} \quad (1)$$

where Y is a proportional factor, j is $\sqrt{-1}$, w is $2\pi f$ and n has the meaning of a phase shift [14]. Often a CPE is used in a model in place of a capacitor to compensate for non-homogeneity in the system. To describe the behaviour of impedance spectra at low frequencies an exponent α is introduced in the expression for the Warburg impedance. Several models and expressions are used to describe this characteristic behaviour of conducting polymer, but the finite-element Warburg impedanceis expressed by

$$W_0 = \frac{R_w \coth(jws)^{\alpha}}{(jws)^{\alpha}} \quad (2)$$

where $s = \lambda^2/D$, with λ as the thickness of the diffusion layer, D the diffusion coefficient of the species involved and R_w is the diffusional resistance. This created the overall equivalent circuit model shown in Fig. 10. As an example of the accuracy of this circuit, parameter values for uncoated 304 stainless steel, PANI and PANI + PVA are given in Tables 2–4, respectively. The error of these parameters were lower than 3%. The R_{ct} values in these equivalent circuits, shown in Figs. 6–9 are equivalent to the R_p values plotted in Fig. 4. However, from Figs. 6–9, it is clear that the smallest R_{ct} value, i.e. the system with the highest corrosion rate, is shown by the PANI-containing coatings, whereas data plotted in Fig. 4 show that this system is the one with the lowest corrosion rate. Beck et al. [17], using PPY onto steel in 0.5 M H_2SO_4 attributes this small semicircle in the impedance spectra to a porous oxalate iron. Koene et al. [12], however, using PPY onto steel in 0.1 M Na_2SO_4, attribute this small R_{ct} values of the polymeric coatings to the conductivity of the polymer. The R_{ct} values reported by Koene lied between 3 and 10 Ω, which are very similar to our values (see Figs. 6–9). The increase in the

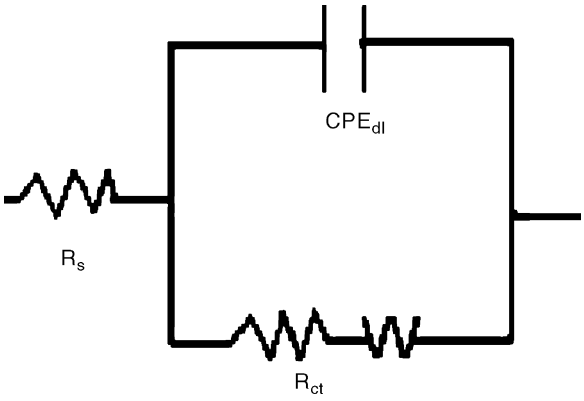

Fig. 10. Equivalent electric circuit used to simulate the impedance results of the different coating systems.

Table 2
Values for the parameters of the electrical circuit used to simulate the impedance data for uncoated 304 SS

t(h)	R_s (Ω)	CPE$_{dl}$		W_0			R_{ct} (Ω)
		Y_0 (Ω^{-1} s^n)	n	R_w (Ω)	s	α	
1	0.58	0.00031	0.9	12.52	0.17	0.35	9.26
2	0.69	0.0011	0.89	11.11	4.89	0.28	21.58
3	0.69	0.0012	0.89	12.49	18.52	0.24	26.5
4	0.7	0.0013	0.89	22.33	109.9	0.15	36
8	0.72	0.0014	0.88	31.1	202.3	0.11	54
16	0.7	0.0017	0.88	40.8	305.6	0.08	63
24	0.67	0.002	0.88	50.7	405.9	0.06	77

Table 3
Values for the parameters of the electrical circuit used to simulate the impedance data for the PANI coating

t (h)	R_s (Ω)	CPE$_{dl}$		W_0			R_{ct} (Ω)
		Y_0 (Ω^{-1} s^n)	n	R_w (Ω)	s	α	
1	0.64	0.0004	0.84	5.1E−7	8.5E−9	0.47	2.37
2	0.63	0.0005	0.83	8.1E−4	2.1E−5	0.47	3.36
3	0.63	0.00054	0.83	2.2E−4	5.4E−6	0.48	3
4	0.63	0.00057	0.82	2.2E−4	6E−6	0.48	2.9
8	0.62	0.00057	0.82	4.6E−3	1.2E−4	0.47	3.1
16	0.62	0.00056	0.81	4.4E−3	1.1E−4	0.48	2.9
24	0.63	0.0053	0.81	8.4E−4	1.9E−4	0.49	2.4

Table 4
Values for the parameters of the electrical circuit used to simulate the impedance data for the PANI + PVA coating

t (h)	R_s (Ω)	CPE_{dl}		W_0			R_{ct} (Ω)
		Y_0 (Ω^{-1} s^n)	n	R_w (Ω)	s	α	
1	0.51	0.0005	0.88	8.4E−7	1.6E−8	0.44	1.02
2	0.51	0.00076	0.85	1.2E−6	1.8E−6	0.44	1.1
3	0.51	0.0006	0.86	1.0E−4	1.1E−5	0.44	1.17
4	0.51	0.0006	0.86	5.0E−4	1.12E−5	0.44	1.18
8	0.51	0.0006	0.86	5.4E−4	7.9E−6	0.44	1.19
16	0.51	0.00058	0.87	9.9E−1	1.9E−5	0.43	1.06
24	0.51	0.00049	0.88	6.3	9.66E−6	0.43	1.02

R_{ct} values with time on the semicircles for the PPY-containing coatings in Figs. 6 and 7, may be related to the reduction of polypirrole as the subsequent loss of available charge transfer sites at the coating/solution interface will increase R_{ct}.

A transition from finite-length diffusion to semi-infinite diffusion is apparent from the Nyquist plots for both PPY coatings shown in Figs. 6 and 7. This strongly suggests that ion diffusion in solution slowly replaces charge diffusion within the polypirrole layer as the dominant charge transfer process as the slope of the low-frequency part in the Nyquist plot approaches 45° towards the end of the tests. The simultaneous increase in R_{ct} and R_w indicates that the reaction rate of the system's Faradic process decreases with time.

3.3. Micrographs

Fig. 11 shows a micrograph of the as-deposited PANI coating whereas Fig. 12 shows this coating after it has been corroded during 24 h in sulfuric acid. The as-deposited coating shows the typical cauliflower-like shape of the PANI polymer, with a particle size between 2 and 3 μm. Once it has been corroded, these particles show now an irregular shape. When PVA is added, this appear homogeneously distributed on the surface of the coating, as seen in Fig. 13, and gives some corrosion protection because the anodic dissolution is not so evident, as can be seen in Fig. 14.

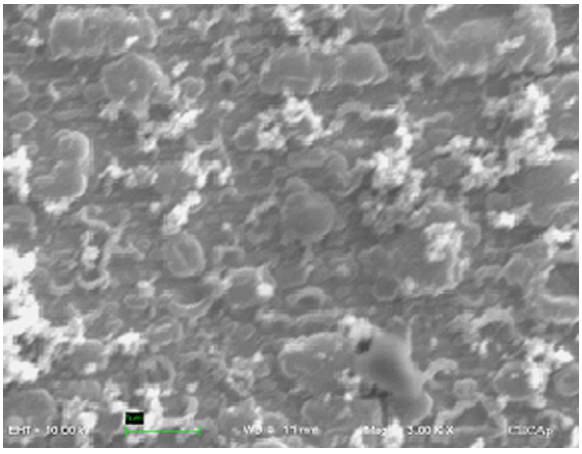

Fig. 12. Micrograph of the corroded PANI coating.

As stated by Koene et al. [12] these kind of polymeric coatings have a high porosity for which a high water uptake is expected. It is likely that local regions are formed with water between the polymeric layer and the substrate. When this occurs dissolution of the substrate is expected. Since these coatings are electrically conductive, transfer of charge between solution and polymer is possible, allowing sulfate ions to enter the polymer layer and eventualy access the substrate surface. This access of corrosive ions may cause the substrate to corrode, producing corrosion

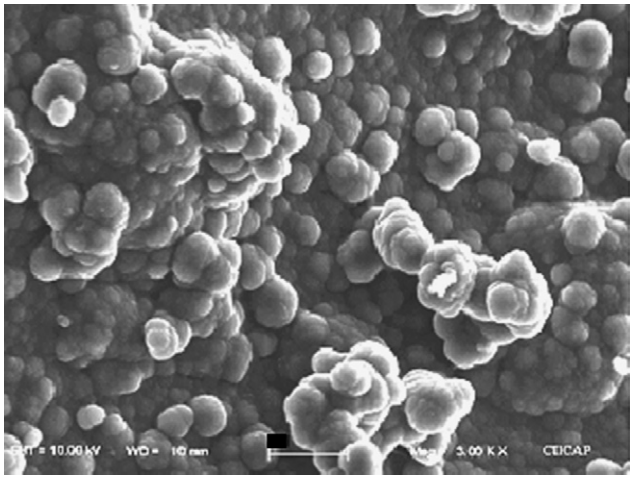

Fig. 11. Micrograph of the as-deposited PANI coating.

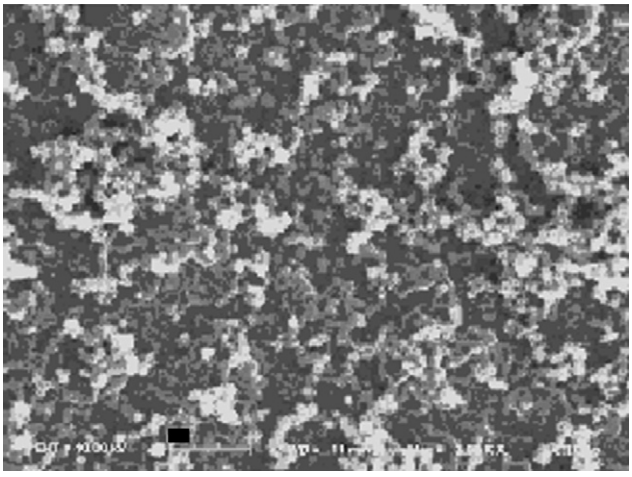

Fig. 13. Micrograph of the as-deposited PANI + PVA coating.

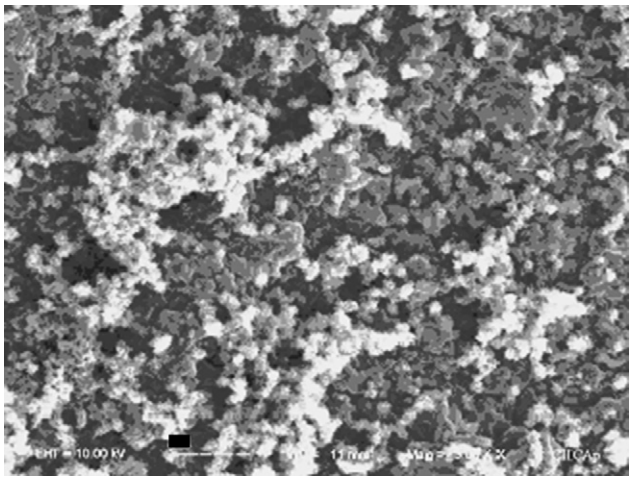

Fig. 14. Micrograph of the corroded PANI + PVA coating.

products. These corrosion products cause the diffusion of charge carriers to be hindered. The additional ions that ingress from the solution increases the conductivity of the coating. Thus, the low-frequency conduction in these coatings observed in the Nyquist diagrams (Figs. 6–9) may be attributed to mobile charges in the polymer backbone and to the mobile ions they contain. In the high frequency range, the development of an additional charge transfer process is visible, possible the onset of substrate corrosion reaction. In the case of PPY-coating (Fig. 6). The R_{ct}, value increases with time, whereas that for PANI coatings it decreases, indicating that overall conduction in the system increases, which, again, may be attributed to the ingress of electrolyte ions. However, the R_{ct}, value for the PANI + PVA system remains constant with time (Fig. 9) similar to the PPY + PVA system (Fig. 7) indicating that PVA gives more protection, because the ingress of the electrolyte ions is less when it is present.

4. Conclusions

A work on the corrosion protection of 304 type stainless steel with the use of conductive polymers, polyaniline (PANI) and polypirrol (PPY) with and without the use of polyvinyl alcohol (PVA) as adhesive in 0.5 M H_2SO_4 at 60 °C has been carried out. It was shown that the free corrosion potential, E_{corr}, of the substrate was made more noble up to 500 mV with the polymeric coatings. The corrosion rate, measured by the linear polarization method, was lowered by using the polymers, but by adding PVA, it was decreased further, one order of magnitude for PPY and up to three orders of magnitude for PANI. Impedance spectra showed that the corrosion mechanism is under a Warburgh-type diffusional process of the electrolyte throughout the coating, and that the uptake of the environment causes the eventual failure of the coating and corrosion of the substrate. The role of the PVA, apart from improving the adhesion of the coating to the substrate, was to block the coating pores, and thus, to decrease the electrolyte diffusion towards the substrate and to corrode it.

References

[1] A. Herman, T. Chaudhuri, P. Spagnol, J. Hydrogen Energy 30 (12) (2005) 1297–1302.
[2] V. Metha, J.S. Cooper, J. Power Sources 114 (2003) 32–53.
[3] A.F. Diaz, K.K. Kamazawa, J. Chem. Soc. Chem. Commun. (1979) 635–638.
[4] K.K. Kamazawa, A.F. Diaz, R.H. Geiss, W.D. Gill, J.F. Kwak, J.A. Logan, J.F. Robalt, G.B. Street, J. Chem. Soc. Chem. Commun. (1979) 854–858.
[5] A.J. Hoeger, Curr. Appl. Phys. 1 (2001) 247–257.
[6] D.W. DeBerry, J. Electrochem. Soc. 132 (1985) 132–139.
[7] B. Wessling, Adv. Mater. 6 (1994) 226–235.
[8] P. Herrasti, P. Ocon, Appli. Surf. Sci. 172 (2001) 276–284.
[9] A.A. Hermass, M. Nakayama, K. Ogura, Electrochim. Acta 50 (2005) 3640–3647.
[10] U. Rammelt, L.M. Duc, W. Pleith, J. Appl. Electrochem. 35 (2005) 1225–1230.
[11] A.K. Iversen, Corr. Sci. 48 (2006) 10361058.
[12] L. Koene, W.J. Hamer, J.H.W. De Wit, J. Appl. Electrochem. 36 (2006) 545–556.
[13] M.E. Nicho, H. Hu, J.G. González-Rodriguez, V.M. Salinas-Bravo, J. Appl. Electrochem. 36 (2) (2006) 153–160.
[14] M.A. Lucio-Garcia, M.A. Smith, J. Power Sources 158 (1) (2006) 397–402.
[15] M. Stearn, A.L. Geary, J. Electrochem. Soc. 105 (1958) 638–643.
[16] D.C. Trivedi, in: H.S. Nalwa (Ed.), Handbook of Organic Conductive Molecules and Polymers, Conductive Polymers: Synthesis and Electrical Properties, vol. 2, John Wiley & Sons Ltd., 1997, pp. 514–520.
[17] F. Beck, R. Michaelis, F. Schloten, B. Zinger, Electrochim. Acta 39 (1994) 229–235.